Journal of Cellular Biochemistry 84:532–544 (2002)

Magnolol Suppresses Proliferation of Cultured Human Colon and Liver Cancer Cells by Inhibiting DNA Synthesis and Activating Apoptosis

Shyr-Yi Lin,[1,2] Jean-Dean Liu,[2] Hui-Chiu Chang,[3] Shauh-Der Yeh,[1] Chien-Huang Lin,[4] and Wen-Sen Lee[1,5]*

[1]Graduate Institute of Medical Sciences, Taipei Medical University, Taipei, Taiwan
[2]Department of Internal Medicine, School of Medicine, Taipei Medical University, Taipei, Taiwan
[3]Department of Physiology, Kaohsiung Medical University, Kaohsiung, Taiwan
[4]Graduate Institute of Biomedical Technology, Taipei Medical University, Taipei, Taiwan
[5]Department of Physiology, School of Medicine, Taipei Medical University, Taipei, Taiwan

Abstract Magnolol, a hydroxylated biphenyl compound isolated from the Chinese herb Hou p'u of *Magnolia officinalis*, has been reported to have anti-cancer activity. In the present study, magnolol at very low concentrations of 3–10 μM inhibited DNA synthesis and decreased cell number in cultured human cancer cells (COLO-205 and Hep-G2) in a dose-dependent manner, but not in human untransformed cells such as keratinocytes, fibroblasts, and human umbilical vein endothelial cells (HUVEC). Magnolol was not cytotoxic at these concentrations and this indicates that it may have an inhibitory effect on cell proliferation in the subcultured cancer cell lines. [^{3}H]thymidine incorporation and flow cytometry analyses revealed that magnolol treatment decreased DNA synthesis and arrested the cells at the G0/G1 phase of the cell cycle. Moreover, the magnolol-induced cell cycle arrest occurred when the cyclin-CDK system was inhibited, just as p21 protein expression was augmented. When magnolol concentration was increased to 100 μM, apoptosis was observed in COLO-205 and Hep-G2 cells, but not in cultured human fibroblasts and HUVEC. COLO-205 cells implanted subcutaneously in nude mice formed solid tumors; subsequent daily i.p. injections of magnolol led to profound regression of these tumors of upto 85%. In these tumors, an increase in the expression of p21 protein level and the occurrence of apoptosis were observed. These findings demonstrate for the first time that magnolol can inhibit the proliferation of tumor cells in vitro and in vivo. J. Cell. Biochem. 84: 532–544, 2002.

Key words: p21; apoptosis; cell cycle; G0/G1 arrest

The occurrence of gastrointestinal cancers has increased strikingly during the last decade. For instance, colorectal cancer is the second leading cause of cancer mortality in Western societies and one of the most common malignancies worldwide [Chinery et al., 1997]. Liver cancer is one of the most prevalent and deadly cancers in the world, causing almost one million deaths annually [Akriviadis et al., 1998]. Although intensive research during the past few years has led to considerable improvement in the treatment and diagnosis at an early stage, for the patient at this time, the prognosis is still not good. Therefore, experimental and clinical investigators continue to search for new therapeutic strategies. One approach, as pursued in this study, seeks to identify medicinal agents capable of retarding the cell cycle and/or activating the cellular apoptotic response in the cancerous cells.

Magnolol, a hydroxylated biphenyl compound isolated from *Magnolia officinalis*, is a widely used Chinese herbal medicine known as Hou p'u. Traditionally, it has been employed to treat such diverse ailments as headache, fever, etc. [Fujita et al., 1973]. Studies using purified magnolol have shown that it can function to scavenge hydroxyl radicals [Haraguchi et al.,

Grant sponsor: Foundations of Jin Lung Yen and Sagittarius Life Science Corp.

*Correspondence to: Wen-Sen Lee, Graduate Institute of Medical Sciences and Department of Physiology, School of Medicine, Taipei Medical University, Taipei 110, Taiwan. E-mail: wslee@tmu.edu.tw

Received 24 July 2001; Accepted 12 October 2001

DOI 10.1002/jcb.10059

1997], inhibit neutrophil adhesion [Shen et al., 1998], suppress the inflammatory response [Wang et al., 1992], inhibit platelet aggregation [Ko et al., 1989], and may also exhibit certain antimicrobial actions [Chang et al., 1998]. Of particular interest for the present study is the magnolol-induced suppression of a cutaneous papilloma, which was induced in mice treated with dimethylbenz[a]anthracene (DMBA) and 12-*O*-tetradecanoylphorbol-13-acetate (TPA) [Konoshima et al., 1991]. Our study was done to investigate any anti-cancer effects of magnolol on human hepatoma and colon carcinoma cells.

MATERIALS AND METHODS

Cell Culture

Four human malignant cell lines (COLO-205, HT-29, Hep-G2, and Hep-3B) and three human primary cells (keratinocytes, fibroblasts, and HUVEC) were used in this study. COLO-205 (CCL-222; American Type Culture Collection) originated from a poorly differentiated human colon adenocarcinoma. Hep-G2 (HB-8065; American Type Culture Collection) was derived from a human hepatoma. HT-29 (HTB-38; American Type Culture Collection) originated from a human colon adenocarcinoma. Hep-3B (HB-8064; American Type Culture Collection) originated from a hepatocellular carcinoma. HUVEC was harvested from the human umbilical vein by enzymatic dissociation as previously described [Jaffe et al., 1973]. Human gingival fibroblasts were harvested by enzymatic dissociation. The cells were grown in RPMI 1640 (for COLO-205 and HT-29), Eagle's minimal essential medium, MEM, (for Hep-G2 and human fibroblasts), or M199 (for HUVEC) supplemented with 10% fetal calf serum (FCS), penicillin (100 U/ml), streptomycin (100 μg/ml), and 0.3 mg/ml glutamine in a humidified incubator (37°C, 5% CO_2). Human keratinocytes were grown in keratinocyte serum free medium (KSFM) supplemented with bovine pituitary extract and epidermal growth factor (EGF). Magnolol (Pharmaceutical Industry, Technology and Development Center, Taiwan) was added at the indicated doses in 0.1% DMSO. For control specimens, the same volume of the 0.1% DMSO without magnolol was added.

[^{3}H]Thymidine Incorporation

As previously described [Jain et al., 1996; Lee et al., 1997], COLO-205 or Hep-G2 at a density of 1×10^4 cells/cm^3 were applied to 24-well plates in growth medium (RPMI 1640 or MEM plus 10% FCS). After the cells had grown to 70–80% confluence, they were rendered quiescent by incubation for 24 h in RPMI 1640 containing 0.04% FCS. Magnolol in 0.1% DMSO or 0.1% DMSO without magnolol (control) in RPMI supplemented with 2% FCS for COLO-205 or MEM with 10% FCS for Hep-G2 was added to the cells at various concentrations and the cultures were allowed to incubate for 21 or 6 h, respectively. During the last 3 h of the incubation with or without magnolol, [^{3}H]thymidine was added at 1 μCi/ml (1μCi = 37 kBq). Incorporated [^{3}H]thymidine was extracted in 0.2 N NaOH and measured in a liquid scintillation counter.

Cell Counting

As a measurement of cell proliferation, the cells at a density of 1×10^4 cells/cm^3 were seeded onto 24-well plates and grown in RPMI 1640 (for COLO-205) supplemented with 2% FCS or MEM (for Hep-G2) supplemented with 10% FCS. Media with and without magnolol were changed daily until cell counting. At various times of incubation, cultures were treated with trypsin-EDTA and the released cells were counted in a Coulter apparatus.

Analysis of DNA Fragmentation

Apoptotic cell death may be documented by various methods, including identification of internucleosomal DNA fragmentation by laddering on DNA gel electrophoresis. Analysis of DNA fragmentation was performed as previously described [Ho et al., 1996]. Briefly, the magnolol and control-treated cells were seeded on 100-mm dishes. The DNA was extracted twice with equal volumes of phenol and once with chloroform-isoamyl alcohol (24:1 v:v), then precipitated with 0.1 volume of sodium acetate, pH 4.8, and 2.5 volumes of ethanol at −20°C overnight, and finally centrifuged at 13,000*g* for 1 h. Genomic DNA was quantitated, and equal amounts of DNA sample in each lane were electrophoresed in a 2% agarose gel. The DNA was visualized by ethidium bromide staining. Genomic DNA isolated from 10 μM terbinafine-treated HT-29 cells showing DNA fragmentation was included in this experiment to serve as a positive control.

Trypan Blue Exclusion Assay

Cell viability was estimated by Trypan blue exclusion assay as previously described [Ho et al., 1997].

Flow Cytometry

As previously described [Lai et al., 1996], the cells were seeded onto 100-mm dishes and grown in RPMI 1640 supplemented with 10% FCS. After the cells had grown to subconfluence, they were rendered quiescent and challenged with 2% FCS. Then, after release using trypsin-EDTA, they were harvested at various times, washed twice with PBS/0.1% dextrose, and fixed in 70% ethanol at 4°C. Nuclear DNA was stained with a reagent containing propidium iodine (50 μg/ml) and DNase-free RNase (2 U/ml) and measured using a fluorescence-activated cell sorter (FACS). The proportion of nuclei in each phase of the cell cycle was determined using established CellFIT (Becton Dickinson, San Jose, CA) DNA analysis software.

Protein Extraction and Western Blot Analysis

The frozen tumor was pulverized in liquid N_2, and then mixed with lysis buffer (Tris-HCl 0.5M, pH 6.8, SDS 0.4%). For cell cultures, the cells were seeded onto 150-mm dishes. After the cells had grown to subconfluence, they were rendered quiescent. The cells were released from quiescence with culture medium supplemented with 2% FCS (for COLO-205) or 10% FCS (for Hep-G2). Magnolol in 0.1% DMSO or 0.1% DMSO without magnolol was added to the cells at various concentrations and the mixture was allowed to incubate for 18 h. The cells were washed with phosphate buffered saline (PBS) and then lysed in lysis buffer (Tris HCl 0.5 M, pH 6.8; SDS 0.4%). Western blot analysis was performed as previously described [Lee et al., 1998]. The protein samples (50 μg/lane) were loaded onto 10% sodium dodecyl sulfate–polyacrylamide gel electrophoresis (SDS–PAGE). The gel electrophoresis was performed at constant 150 V for 3–4 h at 16–18°C. After protein separation, each gel was transferred onto an Immobilon-P membrane. Immunodetection was carried out by probing with proper dilutions of specific antibodies at room temperature for 2 h. Anti-p21, anti-p27, anti-cyclin D1 and D3, anti-CDK2 and CDK4, and anti-PCNA monoclonal antibodies (Transduction, San Diego, CA) and anti-G3PDH monoclonal antibody (Biogenesis, Kingston, NH) were used at a concentration of 1:1,000 dilution. Anti-cyclin A and E polyclonal antibodies (Transduction, San Diego, CA) were used at a concentration of 1:250 dilution. The secondary antibodies, alkaline phosphatase-coupled anti-mouse or anti-rabbit antibody (Jackson, Westgrove PA), was incubated at room temperature for 1 h at a concentration of 1:5,000 or 1:1,000 dilution, respectively. The specific protein complexes were identified using NBT/BCIP (nitro-blue-tetrazolium chloride/bromo-chloro-3-indolyl-phosphate)(Kirkegaard Perry Laboratory, Gaithersburg, MD). In each experiment, membranes were also probed with anti-G3PDH antibody to correct for differences in protein loading.

Immunoprecipitation

Immunoprecipitation was performed as previously described [Ho et al., 1996]. Briefly, CDK2 was immunoprecipitated from 200 μg of protein by using anti-CDK2 antibody (2 μg) and protein A agarose beads (20 μl). The precipitates were washed five times with lysis buffer and once with PBS. The pellet was then resuspend in sample buffer (50 mM Tris, pH 6.8; 100 mM Bromophenol blue, and 10% glycerol) and incubated at 90°C for 10 min before electrophoresis to release the proteins from the beads.

CDK2 Kinase Assay

As previously described [Wu et al., 1996], CDK2 immunoprecipitates from magnolol-treated and control COLO-205 cells were washed three times with lysis buffer and once with kinase assay buffer (50 mM Tris-HCl, pH 7.4, 10 mM $MgCl_2$, and 1 mM DTT). Phosphorylation of histone H1 was measured by incubating the beads with 40 μl of "hot" kinase solution [0.25 μl (2.5 μg) histone H1, 0.5 μl [γ-^{32}P] ATP, 0.5 μl 0.1 mM ATP, and 38.75 μl kinase buffer] at 37°C for 30 min. The reaction was stopped by boiling the sample in SDS sample buffer for 5 min, and the products were analyzed by 12% SDS–PAGE. The gel was dried and visualized by autoradiography.

Antisense Oligonucleotide

The oligonucleotides were designed as previously described (Evdokiou et al., 1999). The antisense oligonucleotide (p21AS) was based on the p21 coding sequence, which is

complementary to the region of the initiation codon (5′-TCCCCAGCCGGTTCTGACAT-3′) and the scramble p21 (p21S) as control (5′-ACCTGTGCTCCGACACGTCT-3′). These oligonucleotides were purchased from Sigma-Genosys, Inc. Phosphorothioate oligodeoxynucleotides were added to the cells at a final concentration of 2 nM at 1 h before the cell was challenged with 2% FCS.

Measurement of Cytosolic-Free Ca^{2+} Concentrations

As previously described [Grynkiewicz et al., 1985], the cells were seeded on coverslips and grown in RPMI 1640 medium supplemented with 10% FCS. After the cells had grown to 60–70% confluence, the medium was changed to RPMI supplemented with 1% FCS for 24 h. The medium was then replaced with a fresh RPMI supplemented with 1% FCS containing 5 μM fura-2/AM (Molecular Probes, Eugene, Oregon), and then incubated for 45 min at 37°C. After washing with Phocal buffer (HEPES 10 mM; NaCl 125 mM; KCl 5 mM; glucose 10 mM; $MgCl_2$ 2 mM; NaH_2PO_4 0.5 mM; $NaHCO_3$ 5 mM; $CaCl_2$ 1.8 mM) for three times, the coverslip was then put into a quartz cuvette containing 1.8 ml of Phocal buffer with a magnetic stir bar. Fluorescence activity was monitored with a fluorescence spectrophotometer (Hitachi F-4500, Tokyo, Japan) at 510 nm with excitation at 340 and 380 nm. $[Ca^{2+}]_i$ was calibrated from the fluorescence intensity using the following equation: $[Ca^{2+}]_i = Kd\ Q\ [(R-R_{min})]/(R_{max}-R)]$, where R represents the fluorescence intensity ratio $F_{\lambda1}/F_{\lambda2}$, in which λ1 (~340 nm) and λ2 (~380 nm) are the fluorescence detection wavelengths for the ion-bound and ion-free indicator, respectively. The values of F_{max}, F_{min}, R_{max}, and R_{min} were obtained at the end of each experiment by the sequential addition of 10 μM ionomycin (BIOMOL Research Laboratories, Plymouth Meeting, PA) and 50 mM ethylene glycol-bis(b-aminoethyl ether) N,N,N′,N′-tetra-acetic acid (EGTA). Q was the ratio of F_{min} to F_{max} at λ2 (~380 nm). The dissociation constant (Kd) was taken as 240 nM.

Tumor Growth Assay

The cells were implanted by injection of a tumor suspension (3×10^6 cells in 0.1 ml RPMI 1640) subcutaneously in the flanks of male nude mice (BALB/c-nu, National Animal Center, Taiwan). Each mouse was implanted with one bolus of tumor cells on day 7. Dosing with magnolol was begun 7 days after implantation (day 0), when the tumors reached ~70 mm^3 in volume. Either the vehicle or magnolol at a dose of 5 mg/50 g, which had been used in various in vivo studies [Watanabe et al., 1983; Hsieh et al., 1998], were given i.p. 5 times/week for 2 weeks. Magnolol was formulated by dissolving it in 5.5% Cremophore RH-40 (BASF, Germany). Tumor volume in mm^3 was calculated by the formula: $\text{volume} = 1/2 \times W^2 \times L$, where W = width and L = length of the tumor [Osborne et al., 1987]. Mice were weighed and sacrificed at day +14, and their general health was monitored during the assay.

TUNEL Staining

TdT-mediated dUTP-biotin nick end labeling was used to detect DNA breaks in apoptotic cells in situ [Tsai et al., 1996]. The tissue sections were rinsed three times with phosphate-buffered saline, incubated in avidin (25 μg/ml in PBS and 0.4% Triton-X 100) for 30 min at room temperature to block endogenous biotin, rinsed three times with PBS, and then incubated in 3% H_2O_2 at room temperature for 10 min. After another three rinses with PBS, the cells were rinsed with TdT buffer and incubated in 50 μl of TdT buffer (10 U of TdT and 0.5 nmol of biotinylated dUTP) at 37°C for 60 min. Biotinylated dUTP incorporated into DNA breaks in the nuclei was detected by an avidin-biotin complex method (DAB/nickel chromogen).

Statistics

All data were expressed as the mean value ± SEM. Comparisons were subjected to ANOVA followed by Fisher's least significant difference test. Significance was accepted at $P < 0.05$.

RESULTS

Inhibition of Cell Proliferation in Magnolol-Treated Cells

In the experiments of Figure 1a,b, COLO-205 and Hep-G2 cells were cultured for 5 days with or without magnolol (3–10 μM), and then the cells were harvested and counted. These data show that minute concentrations of magnolol reduced cell counts by 35–50% in both colon and liver cancer cells. The data of Figure 1c show that treatment with 10 μM magnolol for 6 days had no effect on cell growth in culture of untransformed human keratinocytes, fibroblasts,

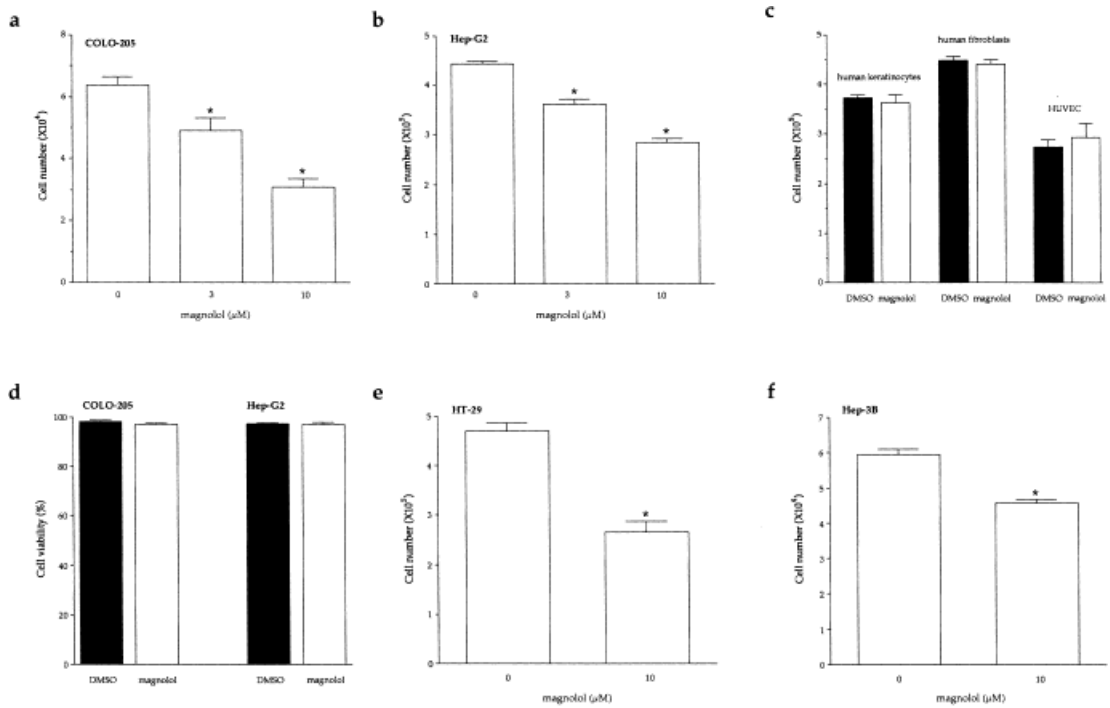

Fig. 1. Effect of magnolol on cell number in human malignant and normal cells. Dose-dependent inhibition of cell growth was observed in COLO-205 (**a**) and Hep-G2 (**b**) cells treated with magnolol. Media with and without magnolol were changed daily until cell counting. Cells were allowed to grow for 5 days after DMSO or magnolol treatment. **c**: Treatment with magnolol at 10 μM concentration for 6 days does not affect growth of untransformed human keratinocytes, fibroblasts, and HUVEC. **d**: Treatment of COLO-205 and Hep-G2 cells with 10 μM magnolol for 5 days does not cause cell death. This inhibitory effect of magnolol on growth was also observed in HT-29 (**e**) and Hep-3B (**f**). Six (COLO-205, keratinocytes, and fibroblasts) or three (HUVEC, Hep-G2, HT-29 and Hep-3B) samples were analyzed in each experiment, and values represent the mean ± SEM. Comparisons were subjected to ANOVA followed by Fisher's least significant difference test. Significance was accepted at $P < 0.05$. *Magnolol-treated group different from control group.

and HUVEC. To confirm further that the results of our studies of cell growth inhibition in COLO-205 and Hep-G2 were not due to cell death caused by magnolol treatment, we conducted viability assays by treating the cells with magnolol for 5 days at the maximal dose (10 μM) used in the studies of cell growth inhibition. Trypan blue exclusion assays indicated that there was no significant difference in cell viability between vehicle-treated and magnolol-treated cells (Fig. 1d). As illustrated in Figure 1e,f, this inhibitory effect of magnolol on growth was also observed in other transformed cultured cells, such as hepatoma (Hep-3B) and colon cancer (HT-29) cell lines.

Arrest of Cell Cycle in G0/G1

In order to examine further the actions of magnolol on the cell cycle, the cells were switched to media with 0.04% FCS to render them quiescent and to synchronize their cell cycle activities. Then they were returned to media with 2% FCS and, at various times thereafter, they were treated with [^{3}H]thymidine. Figure 2a shows a reduction of the thymidine incorporation into COLO-205 during the S-phase of the cell cycle. Figure 2b shows that magnolol inhibited [^{3}H]thymidine incorporation into COLO-205 cells in a dose-dependent manner to as low as 50% of control values, when magnolol concentration was only 10 μM. Similar inhibition was also observed in Hep-G2 (data not shown). Figure 2c shows a representative fluorescence-activated cell sorter (FACS) analysis of DNA content after 18 h release from quiescence at the time of the thymidine incorporation peak by incubation in culture media supplemented with 2% FCS and DMSO or magnolol. The data reveal that magnolol induced a significant accumulation of cells in the G1-phase of the cell cycle, suggesting that the observed growth inhibitory effect of magnolol was due to an arrest of DNA replication, thereby, inhibiting further progress in the cell cycle.

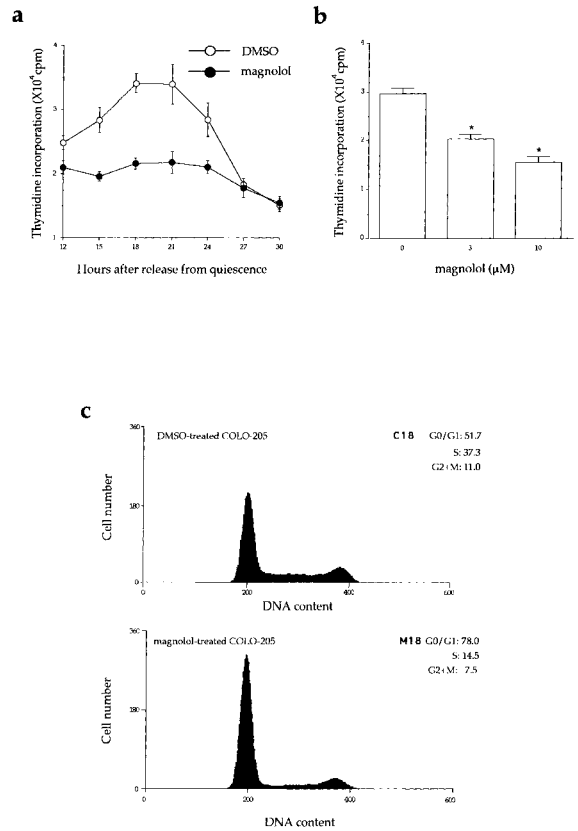

Fig. 2. Effect of magnolol on cell cycle in human malignant cells. **a**: [^{3}H]Thymidine incorporation after cells were released from quiescence by incubation in culture media supplemented with 2% FCS and 0.1% DMSO (open dot) or 10 μM magnolol (solid dot). **b**: Dose-dependent inhibition of [^{3}H]thymidine incorporation in COLO-205 by magnolol. Cultures were incubated with magnolol for 21 h, and [^{3}H]thymidine was added only for the last 3 h of this incubation. **c**: FACS analysis of DNA content after 18 h release from quiescence by incubation in culture media supplemented with 2% FCS and 0.1% DMSO (C18) or 50 μM magnolol in 0.1% DMSO (M18). Percentage of cells in G0/G1, S, and G2/M phases of the cell cycle determined using established CellFIT DNA analysis software is shown in the right upper corner.

Alterations in Cell Cycle Activity

Observation of intracellular events associated with the progression of cell cycle activity have suggested that coordinated successive activation of certain CDKs occurs late in the G1-phase and is instrumental in the transition from the G1- to the S-phase [Hunter and Pines, 1994; Morgan, 1995]. This CDK activation is in turn modulated by association with a number of regulatory subunits called cyclins, and with a group of CDK-inhibitory proteins designated CKIs [Sherr and Roberts, 1995]. Among these CKIs are two known as p21 and p27. Cyclins have been identified as cyclins A, D1, D3, and E. The most common cyclin-dependent-kinases are designated CDK2 and CDK4. In our study of this complex of regulatory factors, we have extracted proteins from COLO-205 and Hep-G2 human cancer cells in culture. The extracted

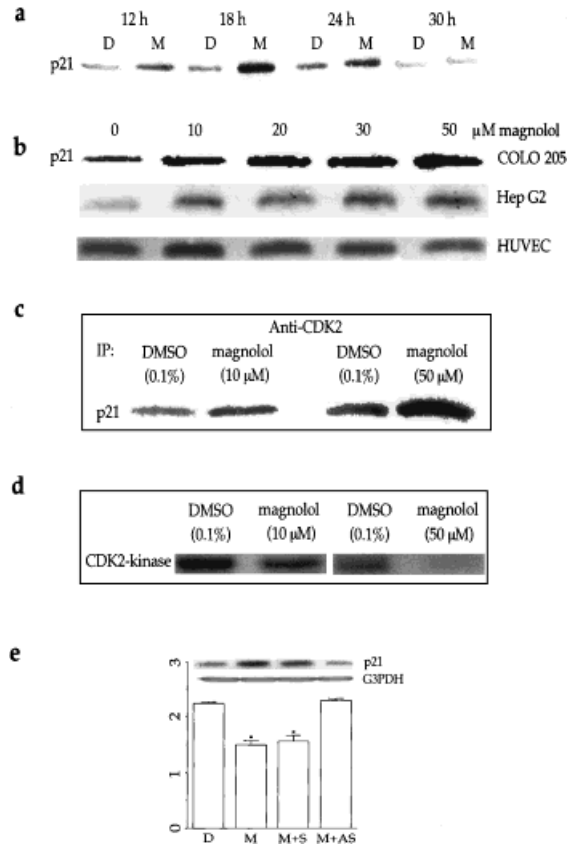

Fig. 3. Effect of magnolol on p21 protein levels, p21-CDK2 association, and CDK2 kinase activity. **a**: The time course of p21 change of COLO-205 in response to magnolol (50 μM) treatment. **b**: Magnolol dose-dependently increases p21 level in COLO-205 and Hep-G2, but not in HUVEC. Proteins were extracted from cultured cells and probed with proper dilutions of specific antibodies. **c**: Dose-dependent upregulation of p21-CDK2 association in COLO-205 by magnolol. CDK2 was immunoprecipitated by anti-CDK2 antibody, and p21-CDK2 association was detected by anti-p21 antibody. **d**: Dose-dependent inhibition of CDK2 kinase activity by magnolol. **e**: Antisense p21 oligonucleotide abolished the magnolol-mediated increase of p21 protein level and decrease of thymidine incorporation. Antisense or scramble p21 was added to COLO-205 at a final concentration of 2 nM at 1 h before the cell was challenged with 2% FCS and magnolol treatment. Cultures were incubated with magnolol for 21 h and [^{3}H]thymidine was added only for the last 3 h of this incubation. Values are mean ± SE (n = 6). Comparisons were subjected to Student's *t*-test. Significance was accepted at $P < 0.05$. *M or M + S-treated group different from DMSO-treated group. D, 0.1% DMSO; M, 10 μM magnolol. S, scramble p21 oligonucleotide; AS, antisense p21 oligonucleotide.

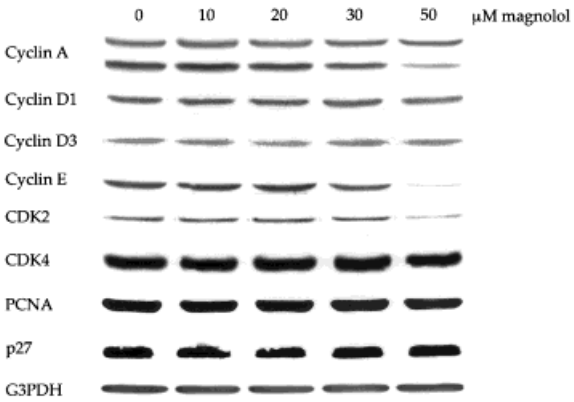

Fig. 4. Effect of magnolol on cyclin, and CDK protein levels. Protein was extracted from the cultured COLO-205 at 18 h after magnolol treatment and probed with proper dilutions of specific antibodies. Magnolol at a range of concentrations (10–30 μM) did not induce any significant changes of the levels of cyclin A, D1, D3 and E, CDK2, CDK4, p27, and PCNA. However, treatment of COLO-205 with magnolol at a concentration of 50 μM for 18 h did induce downregulation of cyclin A and E as well as CDK2, but no change in cyclin D1 and D3, CDK4, p27, and PCNA. Membrane was probed with anti-G3PDH antibody to verify equivalent loading.

proteins were analyzed by gel electrophoresis as described in Materials and Methods.

As illustrated in Figure 3a, treatment of COLO-205 with magnolol resulted in an increase in p21, but not p27 (Fig. 4); the increase was maximal by 18 h after treatment. This upregulation was in a dose-dependent manner (Fig. 3b). Similar results were observed using Hep-G2 cells (Fig. 3b). In contrast, at a dose as high as 50 μM, magnolol did not alter the p21 in untransformed HUVEC (Fig. 3b). In accord with the established notion that p21 is a CDK inhibitor, we found in magnolol-treated cells that the formation of the p21-CDK2 complex was increased (Fig. 3c) and the assayable CDK2 kinase activity was decreased (Fig. 3d). In contrast, the formation of the p21-CDK4 complex was not changed (data not shown). We concluded that such decreased CDK2 activity could account (in part at least) for the impairment in the transition from G1- to S-phases. Finally, to show that in the magnolol-treated cells, increased p21 expression correlated with decreased DNA synthesis activity, the experiment illustrated in Figure 3e was carried out. Thus, in the sample labeled M for magnolol-treated, the p21 electrophoretogram band was increased in intensity, while ^{3}H-thymidine incorporation was reduced by about 30%. Sample M + AS was treated with a p21 antisense oligonucleotide (AS), which blocked the expression of p21. Consequently, in this sample, p21 level did not increase and the magnolol addition to sample M + AS failed to induce the decreased ^{3}H-thymidine incorporation, which was evident in the M (magnolol added) sample.

In order to determine whether the changes of the levels of cyclins and CDK2 were also involved in the magnolol-induced reduction of CDK2 kinase activity, we examined cyclin and CDK protein levels in response to magnolol treatment. Magnolol at concentrations of 10–30 μM did not induce any significant changes of the levels of cyclin A, D1, D3 and E, CDK2, CDK4, p27, and proliferating cell nuclear antigen (PCNA). However, at a concentration of 50 μM, cyclin A and E as well as CDK2 were downregulated (Fig. 4).

Elevation of the Cytosolic-Free Ca^{2+} Is Involved in the Magnolol-Mediated Increase of p21 and Decrease of Thymidine Incorporation in COLO-205

Previous study in rat neutrophils has shown that magnolol induced an increase in cytosolic-free Ca^{2+} via inositol trisphosphate pathway [Wang and Chen, 1998]. Accordingly, we further investigated the possible involvement of cytosolic-free calcium in the magnolol-mediated increase of p21 in COLO-205. The intracellular fura-2/AM fluorescence activity (an indicator of cytosolic-free calcium concentration) in COLO-205 cells treated with or without magnolol was examined. Figure 5a showed an initial rapid spike with sustained high $[Ca^{2+}]_i$ curve in the magnolol-treated COLO-205. The magnolol-induced elevation of $[Ca^{2+}]_i$ occurred in a rapid and dose-dependent manner. Pretreatment of COLO-205 cells with 1,2-bis(2-aminophenoxy)-ethane-N,N,Ní,Ní-tetraacetic acid acetoxymethyl ester (BAPTA/AM, an intracellular chelator) reversed the magnolol-induced suppression of thymidine incorporation (Fig. 5b), suggesting that the magnolol-induced elevation of $[Ca^{2+}]_i$ was involved in the magnolol-induced antiproliferation. Moreover, pretreatment of COLO-205 with 1-[6-[[(17β)-3-methoxyestra-1,3,5(10)-trien-17-yl]amino]hexyl]-1 *H*-pyrrole-2,5-dione (U73122, phospholipase C inhibitor) at a dose of 1 μM, which inhibits the hydrolysis of phosphatidylinositol biphosphate (PIP2) to inositol triphosphate (IP3) and blocked magnolol-induced increase of $[Ca^{2+}]_i$ (data not shown), abolished the magnolol-induced p21 protein

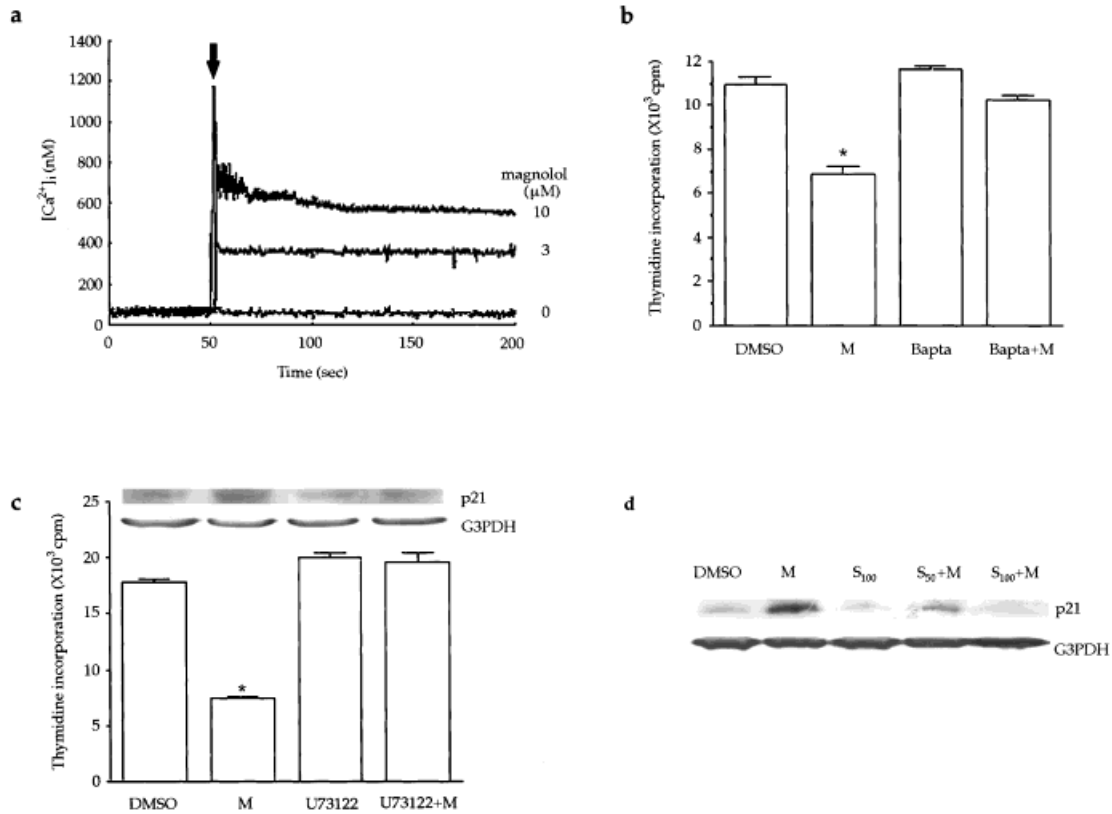

Fig. 5. Elevation of cytosolic-free calcium was involved in the magnolol-induced p21 induction and antiproliferation in COLO-205. **a**: Dose-dependent elevation of $[Ca^{2+}]_i$ in COLO-205 by magnolol (arrow) in the fura-2/AM loaded COLO-205 cells. Vehicle treatment (0 μM magnolol) did not cause any elevation of $[Ca^{2+}]_i$. **b**: Intracellular Ca^{2+} chelator, BAPTA/AM, abolished the magnolol-induced decrease of thymidine incorporation. U73122 and BAPTA/AM were added to COLO-205 at a final concentration of 1 μM at 30 min before the cells were challenged with 2% FCS and magnolol treatment. *Magnolol-treated group different from control (DMSO) group. M, 10 μM magnolol. **c**: Phospholipase C inhibitor, U73122, abolished the magnolol-mediated increase of p21 protein level and decrease of thymidine incorporation. **d**: Staurosporine abolished the magnolol-mediated increase of p21 protein level. Staurosporine was added to COLO-205 at 30 min before the cell was challenged with 2% FCS and magnolol treatment. P21 and G3PDH were detected after 18 h of incubation. DMSO, 0.1% DMSO; M, 50 μM magnolol; S50, 50 nM staurosporine; S100,100 nM staurosporine.

elevation and inhibition of thymidine incorporation (Fig. 5c). These data suggested that magnolol induced an IP3-dependent elevation of free cytosolic Ca^{2+}, which in turn, caused an increase of p21 protein level and an inhibition of DNA synthesis in COLO-205. Since, it has been demonstrated that elevation of intracellular calcium can activate protein kinase C (PKC) [Oancea and Meyer, 1998], we further examined whether PKC pathway was involved in the magnolol-induced p21 expression in COLO-205. Pretreatment with PKC inhibitor, staurosporine, dose-dependently reversed magnolol-induced p21 protein expression (Fig. 5d), suggesting that the PKC pathway was involved in the magnolol-induced p21 protein expression in COLO-205 cells.

Magnolol-Induced Inhibition of Cell Proliferation Is Reversible

We also examined the reversibility of the magnolol-induced inhibition of cell proliferation. Treatment of the COLO-205 (Fig. 6a) and Hep-G2 (Fig. 6b) cells with magnolol (10 μM) for 6 days induced a 55% reduction of cell number as compared with the cells treated with 0.1% DMSO. However, treatment of the cells with magnolol (10 μM) for 3 days followed by 0.1% DMSO without magnolol for an additional 3 days induced only 25% inhibition as compared with the cells treated with 0.1% DMSO for 6 days. These results suggest that the magnolol-induced cell growth inhibition was largely reversible.

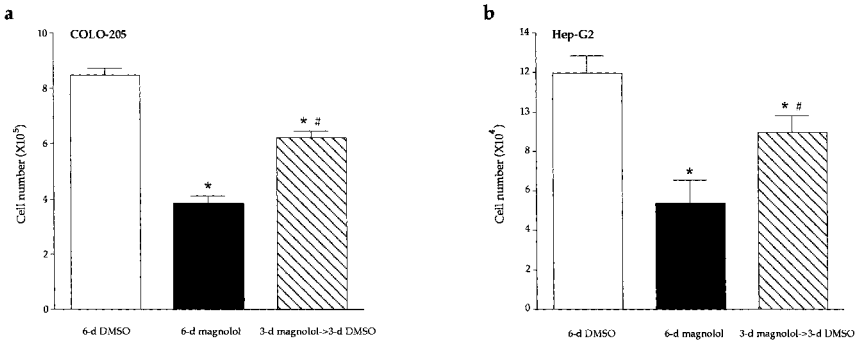

Fig. 6. Reversibility of the magnolol-induced inhibition of cell proliferation. Magnolol-induced inhibition of COLO-205 (**a**) and Hep-G2 (**b**) cell proliferation was reversed by removal of magnolol. Open columns, the cells were treated with 0.1% DMSO for 6 days; solid columns, the cells were treated with 10 μM magnolol for 6 days; striped columns, the cells were treated with 10 μM magnolol for 3 days and then the medium was replaced with 0.1% DMSO without magnolol for an additional 3 days. Six samples were analyzed in each experiment. *6-d magnolol-treated group different from control (6-d DMSO) group and 3-d magnolol + 3-d DMSO-treated group. #3-d magnolol + 3-d DMSO group different from 6-d magnolol-treated group and control group.

Magnolol Effect on DNA Fragmentation

The particular evidence for the occurrence of apoptosis includes the fragmentation of DNA as illustrated in Figure 7. The cells were grown in RPMI 1640 (for COLO-205) or MEM (for Hep-G2) supplemented with 10% FCS and then treated with 100 μM magnolol for various times. Genomic DNAs extracted from magnolol-treated COLO-205 (Fig. 7a) and Hep-G2 (Fig. 7b) were examined by gel electrophoresis and found to display the DNA ladder patterns characteristic of cells undergoing apoptosis. As shown in Figure 7c,d, control HUVEC and human fibroblasts did not show this DNA ladder pattern.

Magnolol Causes Tumor Regression In Vivo

Given the inhibition by magnolol of the growth of transformed colon cells in culture, we next determined whether administration of magnolol could affect the growth of tumors derived from human colon cancer cells in an in vivo setting. A reduction in tumor volume between mice given magnolol vs. those given vehicle (Cremophore RH-40) was detectable by day + 3, three days after initiation of magnolol treatment. This difference became progressively more conspicuous, with the average tumor volume of magnolol-treated mice at ~15% that of vehicle-treated mice at 14 days of treatment (Fig. 8a–c). Since, retardation of the cell cycle and/or activation of the cellular apoptotic response are two major mechanisms preventing tumor growth, we examined the magnolol effect on the cell cycle and apoptosis occurrence of the solid tumor derived from the implanted COLO-205. The particular evidence for the occurrence of apoptosis in the tumor isolated from the magnolol-treated animal includes the fragmentation of DNA as illustrated in Figure 8d. The content of p21, a CDK-inhibitory protein, was increased in the tumor isolated from the magnolol-treated mouse (Fig. 8e), suggesting that the inhibition of the progression of cell cycle activity was involved in the magnolol-induced tumor regression. As illustrated in Table I, intraperitoneal injection of magnolol at a dose of 100 mg/kg, which has been used in various in vivo studies [Watanabe et al., 1983; Hsieh et al., 1998], did not affect the body weight and was not cytotoxic for the vital organs.

DISCUSSION

The present study was undertaken to examine the anti-cancer effect of magnolol on human cancer cells. Our in vitro studies demonstrated that magnolol at concentrations of 3–10 μM inhibited DNA synthesis and the growth rate of COLO-205 and Hep-G2 cells in a dose-dependent manner, but not in human untransformed cells such as keratinocytes, fibroblasts, and HUVEC. These results were not due to necrotic cell death and indicated that there was an inhibitory effect of magnolol on the mechanisms for cell division in the subcultured cancer cells. Furthermore, when magnolol concentration was increased to 100 μM, apoptosis was observed in

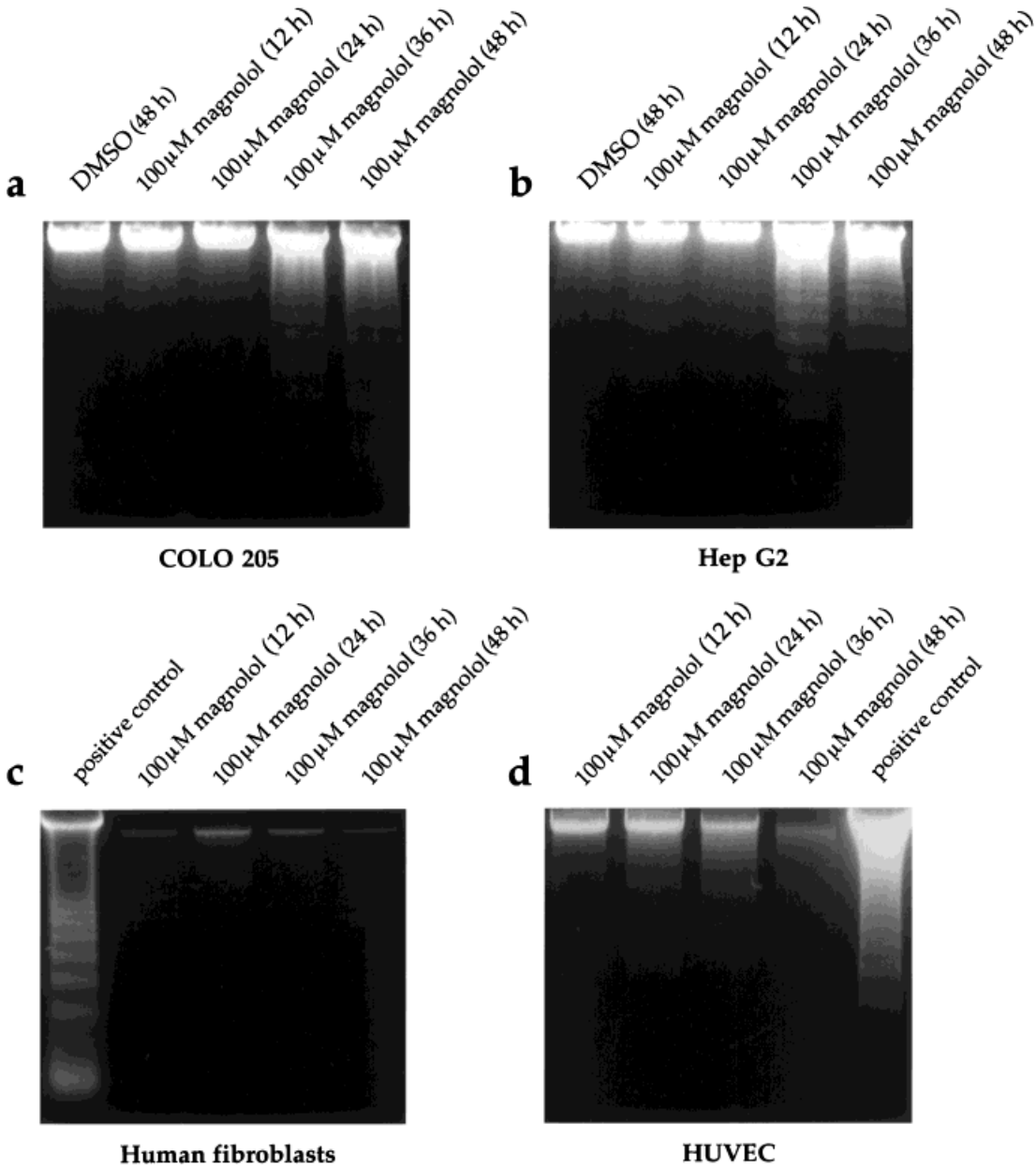

Fig. 7. Magnolol induces DNA fragmentation in human malignant cells. A typical DNA ladder pattern associated with apoptosis was seen in COLO-205 (**a**) and Hep-G2 (**b**) cells treated with 100 μM magnolol for at least 36 h. In contrast, a typical DNA ladder pattern was not observed in human fibroblasts (**c**) or HUVEC (**d**) treated with 100 μM magnolol for up to 48 h. In these experiments, the cells were grown in RPMI 1640 (for COLO-205), MEM (for Hep-G2 and fibroblasts), or M199 (for HUVEC) supplemented with 10% FCS. Genomic DNA isolated from 10 μM terbinafine-treated HT-29 cells were included in this experiment to serve as a positive control.

COLO-205 and Hep-G2 cells, but not in cultured human fibroblasts and HUVEC. In vivo studies show that i.p. administration of magnolol caused a striking and substantial regression of the COLO-205 tumor mass. To our knowledge, this is the first demonstration that magnolol inhibits the growth of colon cancer cells both in vitro and in vivo.

This inhibitory effect of magnolol on growth does not appear to be limited to the COLO-205 and Hep-G2 cells, as similar inhibition has also been observed in other transformed cultured cells, such as Hep-3B and HT-29 (Fig. 1e,f). Importantly, at the doses (3–10 μM) used in our in vitro studies, magnolol was not cytotoxic for the cultured untransformed human cells (such

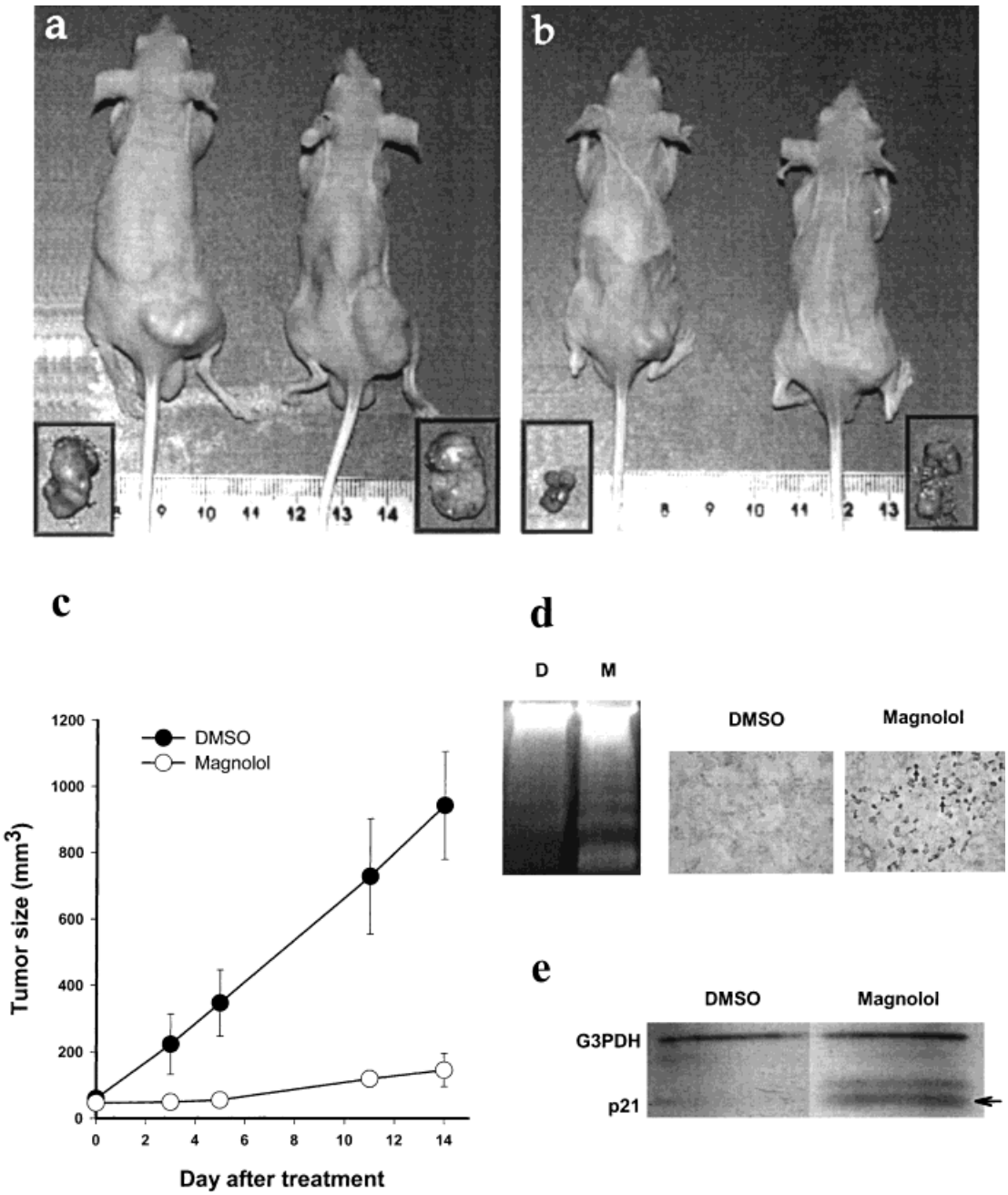

Fig. 8. Magnolol reduces the growth rate of tumors in nude mice. Gross appearance of subcutaneous tumors after treatment with DMSO (**a**) or magnolol (**b**) for 14 days. Insets show the isolated tumors. **c**: Average tumor volume of DMSO-treated (open circles, n = 5) vs. magnolol-treated (filled circles, n = 4) nude mice. Mice were injected subcutaneously with COLO-205 cells at day −7. At day 0, mice were injected intraperitoneally with DMSO or magnolol (100 mg/kg) 5 times/week for 2 weeks. **d**: Induction of apoptosis by magnolol in COLO-205 tumor as shown by DNA fragmentation using electrophoresis of genomic DNA (left panel) and DNA breaks stained in situ by the TdT-mediated dUTP-biotin nick end labeling methods (right panel). Arrows indicate representative apoptotic cells. **e**: Western blot analysis of p21 protein levels in COLO-205 tumor. COLO-205 tumors were harvested for protein extraction at 14 days after DMSO or magnolol treatment. P21 (indicated by arrow) protein levels were quantified, and p21 signals were corrected against those for G3PDH to equalize loading sample size.

as keratinocytes, fibroblasts, and HUVEC), nor did the magnolol have any effect on cell proliferation in these cultures. Moreover, magnolol at a concentration of 100 μM caused the occurrence of apopotsis in COLO-205 and Hep-G2, but not in cultured human fibroblasts and HUVEC. In the animal study, intraperitoneal injection of magnolol at a dose of 100 mg/kg,

TABLE I. Effect of 14-Day Magnolol Treatment on the Weight (g) of Body Organs

	0.1% DMSO-treated (n = 5)	100 mg/kg magnolol-treated (n = 4)
Body	18.500 ± 0.640	17.470 ± 0.530
Heart	0.103 ± 0.004	0.100 ± 0.007
Lung	0.140 ± 0.004	0.130 ± 0.021
Liver	1.310 ± 0.130	1.150 ± 0.014
Kidney	0.340 ± 0.039	0.330 ± 0.012
Intestine	0.061 ± 0.007	0.077 ± 0.011
Spleen	0.098 ± 0.012	0.090 ± 0.019

Values represent the mean ± SEM.

which has been used in various in vivo studies (Watanabe et al., 1983; Hsieh et al., 1998), was not cytotoxic for the vital organs (Table I). Thus, this magnolol extracted from magnolia tree bark seems to possess a selective suppressive action on several malignant cell types.

By thymidine incorporation and flow cytometry analyses, we demonstrate that magnolol at low concentrations (3–10 μM) induced retardation and reduction of COLO-205 and Hep-G2 cells entrance into the S-phase. Cell cycle progression is regulated by successive, coordinated activation of CDKs [Hunter and Pines, 1994; Morgan, 1995], whose activity is controlled by their association with a series of regulatory subunits called cyclins and a group of CDK-inhibitory proteins designated CKIs [Sherr and Roberts, 1995]. Among these CKIs are two known as p21 and p27. Cyclin A-CDK2 and cyclin E-CDK2 complexes form late in the G1 phase as cells prepare to synthesize DNA [Lees, 1995], and formation of the cyclin E complex is a rate-limiting step in the G1/S transition [Sherr, 1993]. By gel electrophoresis and TUNEL staining analyses, we also demonstrate that magnolol in a higher concentration (100 μM) caused apoptosis in COLO-205 and Hep-G2 cells. Apoptosis is a cell suicide mechanism that requires specialized cellular machinery. The central component of this machinery is a proteolytic system involving caspases, a highly conserved family of cysteine proteinases with specific substrates [Thornberry and Lazebnik, 1998]. Observation of an increased expression of p21 protein (Fig. 7d) and the occurrence of apoptosis (Fig. 7e) in the solid tumor isolated from the magnolol-treated mouse suggests that both cell cycle inhibition and apoptotic cell death contribute to the magnolol-induced tumor regression. These findings might explain why magnolol can induce a profound regression (85–90% inhibition) of the solid tumor derived from subcutaneous implantation of COLO-205 cells, while there is only 35–50% growth inhibition in cultured malignant cell lines.

Although the primary mode of action of magnolol remained obscure, our results suggested that cell membrane associated inositol trisphosphate signaling pathway was involved in the magnolol-induced elevation of $[Ca^{2+}]_i$ and increase of p21 protein level. Binding of calcium to PKC single C2- or diacylglycerol to tandem C1-domains has been demonstrated to release the pseudosubstrate inhibitory domain, which in turn, activates the PKC isoforms [Newton, 1995; Quest, 1996]. PKC activation has been associated with p21 expression and growth inhibition of A431 [Toyoda et al., 1998] and IEC-18 [Frey et al., 1997] cells. Our results indicated that PKC pathway was also involved in the magnolol-induced p21 induction in COLO-205 cells.

The experimental findings presented in this paper introduce our basic observations that this herbal "magnolol" can specifically inhibit cancer cell proliferation and induce apoptosis in cancer cells both in cell cultures and also in subcutaneous sites in mice. Although animal studies of magnolol-mediated anti-tumoral action are still ongoing, the findings from the present in vitro and in vivo studies in magnolol anti-cancer effect suggest the potential applications of magnolol in the treatment of human cancer.

ACKNOWLEDGMENTS

We thank Professor Winton Tong (University of Pittsburgh, PA) and Professor Ling-Ru Lee (University of California-Berkeley, CA) for critical reviews of the paper, Dr. Chien-Huang Lin (Taipei Medical University, Taipei, Taiwan) for valuable discussion, and Dr. How Tseng (Taipei Medical University, Taipei, Taiwan) for editorial assistance.

REFERENCES

Akriviadis EA, Llovet JM, Efremidis SC, Shouval D, Canelo R, Ringe B, Meyers WC. 1998. Hepatocellular carcinoma. Br J Surg 85:1319–1331.

Chang B, Lee Y, Ku Y, Bae K, Chung C. 1998. Antimicrobial activity of magnolol and honokiol against periodontopathic microorganisms. Planta Med 64:367–369.

Chinery R, Brockman JA, Peeler MO, Shyr Y, Beauchamp RD, Coffey RJ. 1997. Antioxidants enhance the cytotoxicity of chemotherapeutic agents in colorectal cancer: A p53-independent induction of p21WAF1/CIP1 via C/EBPβ. Nat Med 3:1233–1241.

Evdokiou A, Raggatt LJ, Atkins GJ, Findlay DM. 1999. Calcitonin receptor-mediated growth suppression of HEK-293 cells is accompanied by induction of p21WAF1/CIP1 and G2/M arrest. Mol Endocrinol 13: 1738–1750.

Frey MR, Saxon ML, Zhao X, Rollins A, Evans SS, Black JD. 1997. Protein kinase C isoenzyme-mediated cell cycle arrest involves induction of p21(waf1/cip) and p27(kip) and hypophosphorylation of the retinoblastoma protein in intestinal epithelial cells. J Biol Chem 274:9424–9435.

Fujita M, Itokawa H, Sashida Y. 1973. Studies on the components of *Magnolia obovata* Thunb. 3. Occurrence of magnolol and honokiol in *M. obovata* and other allied plants. Yakugaku Zasshi-J Pharmaceut Soc Jap 93:429–434.

Grynkiewicz G, Poenie M, Tsien RY. 1985. A new generation of Ca^{2+} indicators with greatly improved fluorescence properties. J Biol Chem 260:3440–3450.

Haraguchi H, Ishikawa H, Shirataki N, Fukuda A. 1997. Antiperoxidative activity of neolignans from *Magnolia obovata*. J Pharm Pharmacol 49:209–212.

Ho Y-S, Wang Y-J, Lin J-K. 1996. Induction of p53 and p21/WAF1/CIP1 expression by nitric oxide and their association with apoptosis in human cancer cells. Mol Carcinog 16:20–31.

Ho Y-S, Lee H-M, Mou T-C, Wang Y-J, Lin J-K. 1997. Suppression of nitric oxide-induced apoptosis by *N*-acetyl-L-cysteine through modulation of glutathione, bcl-2, and bax protein levels. Mol Carcinog 19:101–113.

Hsieh M-T, Chueh F-Y, Lin S-M, Chueh F-S, Chen C-F, Lin M-T. 1998. Catecholaminergic mechanisms-mediated hypothermia induced by magnolol in rats. Jpn J Pharmacol 78:501–504.

Hunter T, Pines J. 1994. Cyclins and cancer. II: Cyclin D and CDK inhibitors come of age. Cell 79:573–582.

Jaffe EA, Nachman RL, Becker CG, Minick CR. 1973. Culture of human endothelial cells derived from umbilical veins. Identification by morphologic and immunologic criteria. J Clin Invest 52:2745–2756.

Jain M, He Q, Lee W-S, Kashiki S, Foster LC, Tsai J-C, Lee M-E, Haber E. 1996. Role of CD44 in the reaction of vascular smooth muscle cells to arterial wall injury. J Clin Invest 97:596–603.

Ko F-N, Wu T-S, Liou M-J, Huang T-F, Teng CM. 1989. Inhibition of platelet thromboxane formation and phosphoinositides breakdown by osthole from *Angelica pubescens*. Thromb Haemost 62:996–999.

Konoshima T, Kozuka M, Tokuda H, Nishino H, Iwashima A, Haruna M, Ito K, Tanabe M. 1991. Studies on inhibitors of skin tumor promotion, IX. Neolignans from *Magnolia officinalis*. J Nat Prod 54:816–822.

Lai K, Wang H, Lee W-S, Jain MK, Lee M-E, Haber E. 1996. Mitogen-activated protein kinase phosphatase-1 in rat arterial smooth muscle cell proliferation. J Clin Invest 98:1560–1567.

Lee W-S, Harder JA, Yoshizumi M, Lee M-E, Haber E. 1997. Progesterone inhibits arterial smooth muscle cell proliferation. Nat Med 3:1005–1008.

Lee W-S, Jain MK, Arkonac BM, Zhang D, Shaw SY, Kashiki S, Maemura K, Lee S-L, Hollenberg NK, Lee M-E, Haber E. 1998. Thy-1, a novel marker for angiogenesis upregulated by inflammatory cytokines. Circ Res 82: 845–851.

Lees E. 1995. Cyclin dependent kinase regulation. Curr Opin Cell Biol 7:773–780.

Morgan DO. 1995. Principles of CDK regulation. Nature 374:131–134.

Newton AC. 1995. Protein kinase C. Seeing two domains. Curr Biol 5:973–976.

Oancea E, Meyer T. 1998. Protein kinase C as a molecular machine for decoding calcium and diacylglycerol signals. Cell 95:307–318.

Osborne CK, Coronado EB, Robinson JP. 1987. Human breast cancer in the athymic nude mouse: Cytostatic effects of long-term antiestrogen therapy. Eur J Cancer Clin Oncol 23:1189–1196.

Quest AF. 1996. Regulation of protein kinase C: A tale of lipids and proteins. Enzyme Protein 49:231–261.

Shen YC, Sung Y-J, Chen C-F. 1998. Magnolol inhibits Mac-1 (CD11b/CD18)-dependent neutrophil adhesion: Relationship with its antioxidant effect. Eur J Pharmacol 343:79–86.

Sherr CJ. 1993. Mammalian G1 cyclins. Cell 73:1059–1065.

Sherr CJ, Roberts JM. 1995. Inhibitors of mammalian G1 cyclin-dependent kinases. Genes Dev 9:1149–1163.

Thornberry NA, Lazebnik Y. 1998. Caspases: Enemies within. Science 281:1312–1316.

Toyoda M, Gotoh N, Handa H, Shibuya M. 1998. Involvement of MAP kinase-independent protein kinase C signaling pathway in the EGF-induced p21(WAF1/Cip1) expression and growth inhibition of A431 cells. Biochem Biophys Res Comm 250:430–435.

Tsai J-C, Jain M, Hsieh C-M, Lee W-S, Yoshizumi N, Patterson C, Perrella MA, Cooke C, Wang H, Haber E, Schlegel R, Lee ME. 1996. Induction of apoptosis by pyrrolidinedithiocarbamate and *N*-acetylcysteine in vascular smooth muscle cells. J Biol Chem 271:3667–3670.

Wang JP, Chen CC. 1998. Magnolol induces cytosolic-free Ca^{2+} elevation in rat neutrophils primarily via inositol trisphosphate signalling pathway. Eur J Pharmacol 352:329–334.

Wang J-P, Hsu M-F, Raung S-L, Chen C-C, Kuo J-S, Teng C-M. 1992. Anti-inflammatory and analgesic effects of magnolol. Naunyn Schmiedebergs Arch Pharmacol 346: 707–712.

Watanabe K, Watanabe H, Goto Y, Yamaguchi M, Yamamoto N, Hagino K. 1983. Pharmacological properties of magnolol and honokiol extracted from *Magnolia officinalis*: Central depressant effects. Planta Med 49: 103–108.

Wu X, Rubin M, Fan Z, DeBlasio T, Soos T, Koff A, Mendelsohn J. 1996. Involvement of p27KIP1 in G1 arrest mediated by an anti-epidermal growth factor receptor monoclonal antibody. Oncogene 12:1397–1403.